J. Phys. B: At. Mol. Opt. Phys. 25 (1992) 3693-3708. Printed in the UK

Electron capture and ionization in collisions of fast H^+ and He^{2+} ions with magnesium atoms

M B Shah, P McCallion, Y Itoh† and H B Gilbody

Department of Pure and Applied Physics, The Queen's University of Belfast, Belfast, UK

Received 17 February 1992, in final form 18 May 1992

Abstract. A crossed beam technique incorporating time-of-flight spectroscopy and coincidence counting of fast ion-slow ion and electron-slow ion collision products has been used to obtain individual cross sections for electron capture, transfer ionization and pure ionization in collisions involving Mg atoms. Processes involving Mg^{n+} formation for n between 1 and 4 have been considered for both 90-2000 keV amu^{-1} H^+ impact and 43-500 keV amu^{-1} He^{2+} impact. The results extend available data to energies where, in addition to the outer 3s electron, the inner 2s and 2p electrons in Mg are expected to become important. Discrepancies with previous low energy data are believed to reflect, in part, the use of different normalization procedures. While Mg^+ production is dominated by pure ionization in the present energy range, the important role of transfer ionization in the formation of Mg^{2+}, Mg^{3+} and Mg^{4+} ions is clearly demonstrated. Transfer ionization rather than simple charge transfer is shown to provide the dominant contributions to one-electron capture by H^+ and to both one- and two-electron capture by He^{2+} ions.

1. Introduction

In previous measurements in this laboratory we have used a crossed beam technique (cf Shah and Gilbody 1981, 1982, 1983) to study both ionization and electron capture in fast ion-atom/molecule collisions. Slow ionized target products are identified by time-of-flight spectroscopy and counted in coincidence with either the electrons or fast charged analysed product ions from the same events. The method can therefore provide detailed information on the separate collision processes leading to particular ion or atom products. In the present work we have used this general approach to study electron capture and ionization in collisions of H^+ and He^{2+} ions with magnesium atoms at impact energies within the respective ranges 90-2000 and 43-500 keV amu^{-1}.

In our measurements with protons we have obtained separate cross sections ${}_{10}\sigma_{01}$ for the processes of simple charge transfer

$$H^+ + Mg \rightarrow H + Mg^+ \tag{1}$$

and ${}_{10}\sigma_{0n}$ for transfer ionization

$$H^+ + Mg \rightarrow H + Mg^{n+} + (n-1)e \tag{2}$$

for $n = 2$ and 3. The total cross section for one-electron capture σ_{10} may be expressed as $\sigma_{10} = \Sigma_n {}_{10}\sigma_{0n}$ for $n \geqslant 1$.

† Permanent address: Josai University, Saitama 350-02, Japan.

0953-4075/92/173693+16$04.50

We have also obtained cross sections ${}_{10}\sigma_{1n}$ for the pure ionization process

$$H^+ + Mg \rightarrow H^+ + Mg^{n+} + ne. \tag{3}$$

In our measurements with He^{2+} ions we have considered both one and two-electron capture. We have obtained cross sections ${}_{20}\sigma_{11}$ for simple one-electron capture

$$He^{2+} + Mg \rightarrow He^+ + Mg^+ \tag{4}$$

and ${}_{20}\sigma_{1n}$ for transfer ionization

$$He^{2+} + Mg \rightarrow He^+ + Mg^{n+} + (n-1)e \tag{5}$$

for $n = 2$, 3 and 4. The total cross section σ_{21} for one-electron capture may be expressed as $\sigma_{21} = \Sigma_n {}_{20}\sigma_{1n}$ for $n \geqslant 1$. In the case of two-electron capture we have obtained cross sections ${}_{20}\sigma_{02}$ for the simple two-electron capture process

$$He^{2+} + Mg \rightarrow He + Mg^{2+} \tag{6}$$

and ${}_{20}\sigma_{0n}$ for transfer ionization

$$He^{2+} + Mg \rightarrow He + Mg^{n+} + (n-2)e \tag{7}$$

for $n = 3$ and 4. The total cross section σ_{20} for two-electron capture may be expressed as $\sigma_{20} = \Sigma {}_{20}\sigma_{0n}$ for $n \geqslant 2$.

We have also obtained cross sections ${}_{20}\sigma_{2n}$ for the pure ionization process

$$He^{2+} + Mg \rightarrow He^{2+} + Mg^{n+} + ne \tag{8}$$

for $n = 1$ and 2.

The helium-like alkaline-earth atoms provide an interesting case for study in terms of the two outer electrons and the possible participation of inner shell electrons in the collision process. However detailed studies of collisions involving Mg atoms have not been extensive both from the experimental and theoretical point of view. A number of previous measurements of total cross sections for electron capture have been carried out using the simple growth method with an oven to provide a magnesium vapour target with reliance on vapour pressure tables to estimate target thicknesses. In this category are the measurements of the total one-electron capture cross sections σ_{10} for proton impact by Il'in *et al* (1965), Berkner *et al* (1969), Morgan and Eriksen (1979) and DuBois and Toburen (1985) in the respective energy ranges 10–180, 5–70, 1–80 and 2–100 keV amu^{-1}. In addition DuBois and Toburen (1985) have measured total cross sections σ_{21} and σ_{20} for one- and two-electron capture by He^{2+} ions in the respective energy ranges 1.3–67 and 2.7–67 keV amu^{-1}.

More recently DuBois (1986) has used a crossed beam method with coincidence counting of selected fast and slow ion collision products. Measurements were carried out for both proton and helium ion impact within the energy range 2–100 keV amu^{-1} to obtain some individual capture and ionization cross sections. These measurements were normalized to previously measured total one-electron capture cross sections using the oven target approach. The present measurements complement the measurements of DuBois (1986) but are based on both fast ion–slow ion and electron–slow ion coincidence counting. Our results extend the available data to energies where, in addition to the outer 3s electron, the involvement of inner 2s and 2p electrons is expected to become important. In our work, rather than rely on previously measured total electron capture cross sections using the oven target approach (where accurate determination of target thickness is difficult), we have normalized our measurements

by reference to the absolute cross sections for single ionization of magnesium by electrons measured by Freund *et al* (1990) using a fast intersecting beam technique with an estimated accuracy of ±10%.

2. Experimental approach

2.1. General description

The basic experimental arrangement was similar to that used in our previous measurements (cf Shah and Gilbody 1982) so that only the essential features need be described here.

A well collimated beam of H^+ or He^{2+} ions of energy adjustable in the respective ranges 90–1000 and 43–500 keV amu^{-1}, which had been subjected to both momentum and energy analysis (see figure 2 of Shah and Gilbody 1981), was arranged to intersect (at right angles) a thermal energy beam of Mg atoms. The crossed beam region was maintained at a pressure of about 5×10^{-8} Torr. The magnesium beam was derived from the same oven source that was used in our recent studies (McCallion *et al* 1992) of the ionization of magnesium by electron impact. During the measurements the oven was operated at a range of temperatures which produced estimated Mg atom beam densities between 10^{10} and 10^{12} atoms cm^{-2}.

Slow Mg^{n+} ions were extracted from the crossed beam region by a transverse electric field (applied between two high transparency grids) high enough to ensure complete collection and counted by a particle multiplier. Mg^{n+} ions in particular charge states n could be identified and distinguished from signals due to background gas collision products by their different times of flight to the multiplier in accordance with the charge to mass ratios. The primary ion beam was charge analysed by electrostatic deflection beyond the crossed beam region.

In order to obtain detailed information on particular electron capture channels a particle multiplier was used to count selected fast product atoms/ions in specified charge states in delayed coincidence with the slow ions of specified charge states formed from the same events (see figure 1 of Shah and Gilbody 1982). A typical slow ion–fast ion coincidence spectrum is shown in figure 1. The contributions from Mg^+, Mg^{2+}, Mg^{3+} and Mg^{4+} can be seen to be well resolved. No attempt was made to separate the contributions from the isotopes ^{24}Mg, ^{25}Mg and ^{26}Mg which have abundances of 79%, 10% and 11% respectively.

In order to obtain information on the pure ionization processes leading to specified charge states of magnesium slow Mg^{n+} ions and electrons were extracted with high efficiency from the crossed beam region and separately counted by particle multipliers on either side of the crossed beam region. The Mg^{n+} ions arising from ionizing processes could be distinguished from those arising from electron capture without ionization by counting them in delayed coincidence with the electrons from the same events. A typical time-of-flight electron–Mg^{n+} coincidence spectrum is shown in figure 2. The contributions from Mg^+, Mg^{2+}, Mg^{3+} and Mg^{4+} ions can be seen to be well resolved.

2.2. Measuring, calibration and normalization procedure for electron capture cross sections

The cross section σ_n^c for a specific process (which might involve either one- or two-electron capture) leading to Mg^{n+} ions in charge state n may be expressed as

$$\sigma_n^c = S(Mg^{n+})/k(Mg^{n+})k(p)\mu. \tag{9}$$

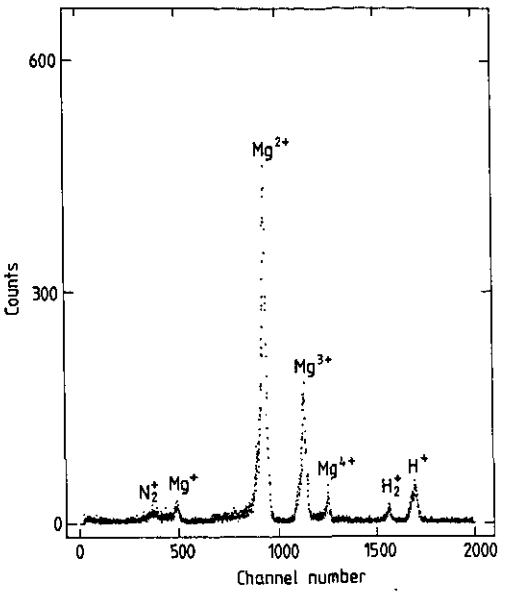

Figure 1. Slow ion–fast product ion coincidence spectrum showing Mg^{n+} ions produced as a result of one-electron capture by 125 keV amu^{-1} He^{2+} ions in collisions with Mg atoms.

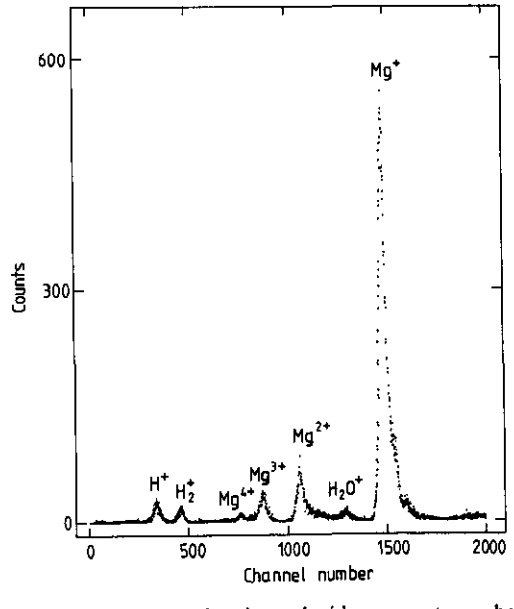

Figure 2. Electron–slow ion coincidence spectrum showing Mg^{n+} ions produced in ionization by 125 keV amu^{-1} He^{2+} ions in collision with Mg atoms.

Here $S(Mg^{n+})$ is the measured slow ion–fast particle coincidence signal per unit primary beam intensity corresponding to the specific capture process; $k(Mg^{n+})$ and $k(p)$ are the respective detection efficiencies of the slow Mg^{n+} ions and fast products of charge exchange formed in the primary beam; μ is the target thickness presented by the Mg atoms in the beam.

Our measured relative cross sections σ_n^c were normalized by reference to our recently measured cross sections for multiple ionization of Mg by electron impact (McCallion *et al* 1992) using a pulsed crossed beam technique which rely on absolute measurements of Freund *et al* (1990) of single ionization of Mg by electron impact. In order to carry out this normalization, we used a technique which we have described previously (Shah *et al* 1987) in which a pulsed electron gun, constructed on a sliding mount within the vacuum chamber, could be substituted for the ion beam in precisely the same position with the target conditions unchanged. The normalization was carried out by comparing Mg^{n+} yields from either an electron beam or a beam of He^{2+} ions. The He^{2+} beam was pulsed (by means of deflector plates in the beam entrance line) with the same mark-to-space ratio as the electron beam corresponding to pulse width of 150 ns and a repetition rate of 10^5 pulses/s. As described previously (Shah *et al* 1987), immediately after the transit of each He^{2+} or electron pulse through the Mg atom beam, slow Mg^{n+} product ions formed in the crossed beam region were extracted by applying a pulsed electric field across the high transparency grids. The Mg^{n+} ions in each charge state n were distinguished by time-of-flight analysis and counted by the particle multiplier.

The cross section $\sigma_n(He^{2+})$ corresponding to the Mg^{n+} yield of specified charge state n (from all processes) for He^{2+} impact may be expressed as

$$\sigma_n(He^{2+}) = S_i(Mg^{n+})/k(Mg^{n+})\mu \tag{10}$$

where $S_i(Mg^{n+})$ is the yield of Mg^{n+} ions per unit ion beam intensity. Similarly the corresponding cross section $\sigma_n(e)$ for electron impact may be expressed as

$$\sigma_n(e) = S_e(Mg^{n+})/k(Mg^{n+})\mu \tag{11}$$

where $S_e(Mg^{n+})$ is the yield of Mg^{n+} ions per unit electron beam intensity.

Using an electron beam energy of 150 eV and our known cross sections (McCallion *et al* 1992) for $\sigma_1(e)$ and $\sigma_2(e)$, we obtained the values of $k(Mg^{n+})\mu$ from equation (11). It was found that the ratio $k(Mg^+)/k(Mg^{2+}) = 1$ to within our measuring accuracy of 4%. The values of $k(Mg^{3+})$ and $k(Mg^{4+})$ should also be same as $k(Mg^{2+})$ and $k(Mg^+)$.

Equations (10) and (11) were used to obtain cross sections $\sigma_2(He^{2+})$ and $\sigma_3(He^{2+})$ for a range of energies up to 110 keV amu^{-1}; it was difficult to pulse the He^{2+} beam at higher energies. These cross sections which correspond to Mg^{2+} and Mg^{3+} production from all electron capture and ionization processes are shown in figure 3. Also shown in figure 3 are our relative values of the cross section sums $({}_{20}\sigma_{12} + {}_{20}\sigma_{02})$ and $({}_{20}\sigma_{13} + {}_{20}\sigma_{03})$ normalized to our values of $\sigma_2(He^{2+})$ and $\sigma_3(He^{2+})$. At energies up to 110 keV amu^{-1}, where any contribution from pure ionization is relatively small, the energy dependence of the two sets of data can be seen to be in very good accord. This normalization procedure allowed the product $k(Mg^{n+})k(p)\mu$ in equation (9) to be determined so that individual cross sections for either H^+ or He^{2+} impact could then be obtained.

Throughout the measurements it was found important to have a reliable continuous indication of the intensity of the Mg atom beam since a constant intensity could not be ensured simply by controlling the oven temperature. A pulsed electron beam from a simple electron gun operating at the fixed energy of 30 eV was arranged to intercept the Mg atom beam at a point beyond the main crossed beam region. The Mg^+ product ions were identified by time-of-flight spectroscopy and recorded by a channeltron and this signal was used to monitor any changes in the Mg atom beam flux.

We had to consider the possibility that the efficiency of the channeltron and the detection efficiency $k(Mg^{n+})$ of the multiplier used to record Mg^{n+} ions might change

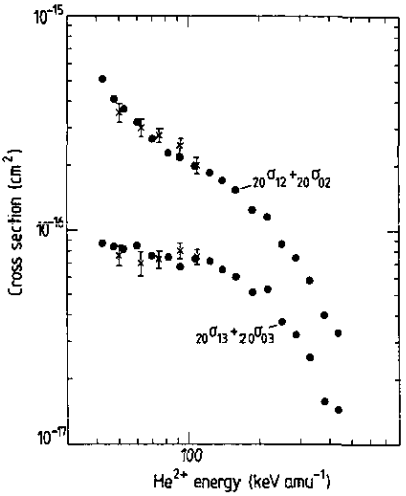

Figure 3. Relative cross sections $({}_{20}\sigma_{12}+{}_{20}\sigma_{02})$ and $({}_{20}\sigma_{13}+{}_{20}\sigma_{03})$ shown (●) normalized to cross sections $\sigma_2(He^{2+})$ and $\sigma_3(He^{2+})$ respectively shown (×) (see text).

due to surface contamination by Mg atoms over the measuring period. In order to monitor any such changes, a very small amount of helium gas was fed into the main vacuum chamber so that a He^+ peak appeared in the time-of-flight spectra (not in figure 1) which could be measured relative to the Mg^+ peak.

2.3. Measuring, calibration and normalization procedure for pure ionization cross sections

Measurements of the electron-Mg^{n+} coincidence signals allow an apparent ionization cross section $\sigma_n^i(X^{z+})$ to be determined where

$$\sigma_n^i(X^{z+}) = S_n/k(Mg^{n+})k(ne)\mu. \tag{12}$$

In this expression, S_n is the electron-slow ion coincidence signal corresponding to n times ionized Mg per unit primary beam current, $k(Mg^{n+})$ is the efficiency of detection of Mg^{n+} ions and $k(ne)$ the efficiency of detection of a group of n electrons; μ is the Mg atom target thickness traversed by the primary ion beam. With $n=1$ in (12), the measured cross section $\sigma_1^i(X^{z+})$ is simply that for the pure ionization processes (3) and (8) corresponding to ${}_{10}\sigma_{11}$ for H^+ impact and ${}_{20}\sigma_{21}$ for He^{2+} impact respectively. However for $n>1$, measured cross sections $\sigma_n^i(X^{z+})$ contain contributions from both pure and transfer ionization processes. Subtraction of our measured transfer ionization cross sections from our measured values of $\sigma_n^i(X^{z+})$ then allows cross sections for the pure ionization processes (3) and (8) to be separately determined.

In order to determine the product $k(Mg^{n+})k(ne)\mu$ in equation (12) we again relied on the absolute cross sections for single ionization of Mg by electrons measured by Freund *et al* (1990) through the data of McCallion *et al* (1992) by comparing signals with a pulsed beam of electrons which could be substituted for the ion beam in precisely the same position with the target conditions unchanged.

For pulsed electron impact, the Mg^{n+} yield $S_n(e)$ (corresponding to a particular value of n) per unit electron current is related to the electron impact ionization cross section $\sigma_n(e)$ through the expression

$$\sigma_n(e) = S_n(e)/k(Mg^{n+})\mu. \tag{13}$$

For a pulsed proton beam the Mg^{n+} yield $S_n(H^+)$ (corresponding to a particular value of n) per unit proton current is related to the cross section $\sigma_n(H^+)$ for Mg^{n+} formation from all ionization and electron capture processes by the expression

$$\sigma_n(H^+) = S_n(H^+)/k(Mg^{n+})\mu. \tag{14}$$

These measurements were used with equations (13) and (14) and our previously measured values of $\sigma_n(e)$ at 150 eV (McCallion *et al* 1992) to obtain normalized values of $\sigma_n(H^+)$ at energies in the range 200–600 keV amu^{-1}. Normalization measurements at higher proton energies were precluded by the limitations of the electronics used to pulse the H^+ beam.

Account has to be taken of the fact that cross sections $\sigma_n(H^+)$ contain contributions from both electron capture as well as ionization. Thus the cross section $\sigma_1(H^+) = ({}_{10}\sigma_{11} + {}_{10}\sigma_{01})$. Normalized values of ${}_{10}\sigma_{11}$ for pure ionization could be derived from $\sigma_1(H^+)$ by subtracting our measured values of ${}_{10}\sigma_{01}$ for simple charge transfer. In fact the contribution of ${}_{10}\sigma_{01}$ to $\sigma_1(H^+)$ is only 0.6% at 200 keV amu^{-1} and decreases rapidly with increasing energy so that $\sigma_1(H^+) \simeq {}_{10}\sigma_{11}$. Since ${}_{10}\sigma_{11} = \sigma_1^i(H^+)$ this normalizing procedure determines the product $k(Mg^+)k(e)\mu$ in equation (12). In figure 4 we show our relative cross sections ${}_{10}\sigma_{11}$ measured in the range 90–2000 keV amu^{-1} fitted to normalized values of ${}_{10}\sigma_{11}$ in the range 200–600 keV amu^{-1}. Cross sections ${}_{20}\sigma_{21}$ for single ionization of Mg by He^{2+} impact could then be determined from $\sigma_1^i(He^{2+}) = {}_{20}\sigma_{21}$.

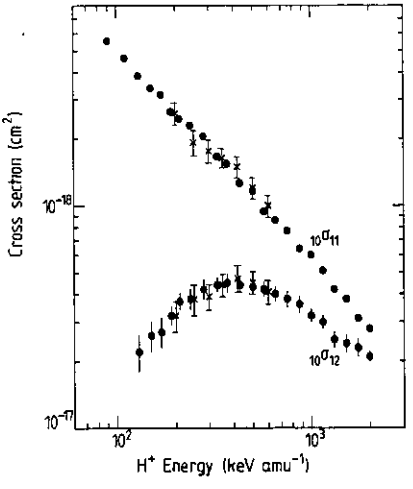

Figure 4. Relative cross sections ${}_{10}\sigma_{11}$ and ${}_{10}\sigma_{12}$ shown (●) fitted to our normalized values ${}_{10}\sigma_{11}$ and ${}_{10}\sigma_{12}$ shown (×) (see text).

In the case of double ionization, in order to obtain cross sections $\sigma_2^i(H^+)$ from equation (12) the product $k(Mg^{2+})k(2e)\mu$ was determined in a similar way to cross sections for single ionization by the use of equations (13) and (14) and our recently measured cross section $\sigma_2(e)$ for electron impact at 150 eV (McCallion *et al* 1992). The cross section $\sigma_2(H^+)$ may be expressed as $\sigma_2(H^+) = ({}_{10}\sigma_{12} + {}_{10}\sigma_{02})$ where cross sections ${}_{10}\sigma_{02}$ are known from the present measurements. Possible contributions from ${}_{10}\sigma_{\bar{1}2}$ corresponding to H^- formation through two-electron capture are known to be negligibly small in the present energy range (Morgan and Eriksen 1979). In figure 4 we show normalized values of ${}_{10}\sigma_{12} = (\sigma_2(H^+) - {}_{10}\sigma_{02})$ obtained in this way in the range

200–600 keV amu^{-1} fitted to our relative values of ${}_{10}\sigma_{12} = (\sigma_2^i(H^+) - {}_{10}\sigma_{02})$ obtained through equation (12) over the range 130–2000 keV amu^{-1}. With the product $k(Mg^{2+})k(2e)\mu$ in equation (12) determined in this way it was then also possible to obtain cross sections ${}_{20}\sigma_{22}$ for ionization by He^{2+} impact.

For triple and quadruple ionization of Mg, in the case of H^+ impact, relative cross sections $\sigma_3^i(H^+)$ and $\sigma_4^i(H^+)$ were too small to be accurately distinguished from the random background signals. For He^{2+} impact, relative cross sections $\sigma_3^i(He^{2+})$ and $\sigma_4^i(He^{2+})$ could be measured, but these are dominated by transfer ionization contributions and contain negligible contributions from the direct ionization cross sections ${}_{20}\sigma_{23}$ and ${}_{20}\sigma_{24}$.

3. Results and discussion

In tables 1–5 are listed our measured cross sections for simple charge transfer, transfer ionization and pure ionization for both H^+ and He^{2+} impact. The uncertainties shown reflect 67% confidence levels based on the degree of reproducibility of the measured values. In addition, all cross sections are subject to uncertainties arising from our normalization procedure estimated to be ±15% for ${}_{10}\sigma_{01}$, ${}_{10}\sigma_{02}$, ${}_{10}\sigma_{03}$, ${}_{10}\sigma_{11}$, ${}_{20}\sigma_{11}$, ${}_{20}\sigma_{12}$, ${}_{20}\sigma_{13}$, ${}_{20}\sigma_{14}$, ${}_{20}\sigma_{02}$, ${}_{20}\sigma_{03}$, ${}_{20}\sigma_{04}$ and ${}_{20}\sigma_{21}$ and ±20% for ${}_{10}\sigma_{02}$ and ${}_{20}\sigma_{22}$.

Table 1. Cross sections ${}_{10}\sigma_{01}$, ${}_{10}\sigma_{02}$ and ${}_{10}\sigma_{03}$ for one-electron capture by H^+ ions in collisions with Mg.

Energy (keV amu^{-1})	${}_{10}\sigma_{01}$ (10^{-17} cm^2)	${}_{10}\sigma_{02}$ (10^{-17} cm^2)	${}_{10}\sigma_{03}$ (10^{-17} cm^2)
90	0.58 ± 0.05	2.42 ± 0.11	0.20 ± 0.02
110	0.41 ± 0.03	2.38 ± 0.13	0.24 ± 0.02
130	0.25 ± 0.02	2.03 ± 0.10	0.20 ± 0.02
150	0.161 ± 0.015	1.88 ± 0.12	0.17 ± 0.02
170	0.118 ± 0.011	1.63 ± 0.09	0.18 ± 0.02
190	0.090 ± 0.007	1.33 ± 0.09	0.140 ± 0.015
210	0.071 ± 0.006	1.21 ± 0.08	0.130 ± 0.010
240	0.051 ± 0.004	0.98 ± 0.06	0.105 ± 0.010
280	0.028 ± 0.002	0.66 ± 0.04	0.066 ± 0.004
330	0.021 ± 0.002	0.48 ± 0.03	0.049 ± 0.003
370	0.0105 ± 0.0015	0.37 ± 0.02	0.042 ± 0.003
430	0.0090 ± 0.0010	0.24 ± 0.02	0.027 ± 0.002
500	0.0049 ± 0.0004	0.155 ± 0.010	0.017 ± 0.002
570	—	0.105 ± 0.010	0.0125 ± 0.0010
650	—	0.069 ± 0.005	0.0073 ± 0.0006
750	—	0.044 ± 0.003	0.0055 ± 0.0004
870	—	0.0231 ± 0.0015	—
1000	—	0.0129 ± 0.0011	—

3.1. Total cross sections for electron capture by H^+ and He^{2+} ions

In figure 5, we show values of total cross sections $\sigma_{10} \simeq \Sigma\, {}_{10}\sigma_{0n}$ (for up to $n = 3$) for one electron capture by protons and $\sigma_{21} \simeq \Sigma\, {}_{20}\sigma_{1n}$ and $\sigma_{20} \simeq \Sigma\, {}_{20}\sigma_{0n}$ (for up to $n = 4$)

Table 2. Cross sections ${}_{10}\sigma_{11}$ and ${}_{10}\sigma_{12}$ for single and double ionization of Mg atoms by H^+ impact.

Energy (keV amu^{-1})	${}_{10}\sigma_{11}$ (10^{-16} cm^2)	${}_{10}\sigma_{12}$ (10^{-17} cm^2)
90	5.55 ± 0.35	—
110	4.64 ± 0.28	—
130	3.86 ± 0.22	2.2 ± 0.4
150	3.37 ± 0.22	2.6 ± 0.4
170	3.15 ± 0.16	2.7 ± 0.4
190	2.64 ± 0.16	3.2 ± 0.3
210	2.45 ± 0.15	3.7 ± 0.3
240	2.29 ± 0.14	3.8 ± 0.4
280	2.05 ± 0.14	4.2 ± 0.4
330	1.66 ± 0.10	4.4 ± 0.3
370	1.54 ± 0.08	4.5 ± 0.4
430	1.26 ± 0.07	4.4 ± 0.3
500	1.16 ± 0.08	4.3 ± 0.3
570	0.94 ± 0.05	4.2 ± 0.3
650	0.86 ± 0.05	4.0 ± 0.3
750	0.77 ± 0.05	3.8 ± 0.3
870	0.64 ± 0.04	3.6 ± 0.3
1000	0.60 ± 0.04	3.2 ± 0.2
1150	0.51 ± 0.03	3.0 ± 0.2
1320	0.42 ± 0.03	2.5 ± 0.2
1520	0.380 ± 0.023	2.4 ± 0.2
1750	0.311 ± 0.023	2.3 ± 0.2
2000	0.280 ± 0.017	2.1 ± 0.2

Table 3. Cross sections ${}_{20}\sigma_{11}$, ${}_{20}\sigma_{12}$, ${}_{20}\sigma_{13}$ and ${}_{20}\sigma_{14}$ for one-electron capture by He^{2+} ions in collisions with Mg.

Energy (keV amu^{-1})	${}_{20}\sigma_{11}$ (10^{-17} cm^2)	${}_{20}\sigma_{12}$ (10^{-17} cm^2)	${}_{20}\sigma_{13}$ (10^{-17} cm^2)	${}_{20}\sigma_{14}$ (10^{-17} cm^2)
42.5	69 ± 5	48.6 ± 2.5	6.2 ± 0.4	—
47.5	41 ± 3	39.6 ± 1.6	6.4 ± 0.3	—
52.5	26 ± 2	35.7 ± 1.3	6.3 ± 0.4	—
60.0	14.1 ± 1.0	31.2 ± 1.3	6.9 ± 0.4	—
70.0	6.1 ± 0.6	26.2 ± 1.1	6.2 ± 0.3	0.75 ± 0.08
82.5	3.5 ± 0.4	22.5 ± 0.9	6.2 ± 0.3	0.87 ± 0.08
92.5	2.6 ± 0.3	21.4 ± 0.9	5.5 ± 0.3	1.03 ± 0.09
108	1.82 ± 0.16	19.6 ± 1.0	6.2 ± 0.4	0.96 ± 0.10
125	1.17 ± 0.10	18.3 ± 0.9	6.1 ± 0.4	1.26 ± 0.15
143	0.96 ± 0.07	16.8 ± 0.8	5.5 ± 0.4	1.08 ± 0.08
163	0.73 ± 0.05	15.2 ± 0.8	5.2 ± 0.4	1.08 ± 0.10
188	0.68 ± 0.07	12.3 ± 0.6	4.5 ± 0.3	0.88 ± 0.10
218	0.55 ± 0.07	11.4 ± 0.8	4.8 ± 0.4	1.06 ± 0.10
250	0.37 ± 0.05	8.6 ± 0.6	3.4 ± 0.4	0.71 ± 0.08
288	0.26 ± 0.04	7.4 ± 0.5	3.0 ± 0.3	0.70 ± 0.08
330	0.11 ± 0.03	5.8 ± 0.4	2.4 ± 0.4	0.46 ± 0.05
380	0.090 ± 0.025	4.0 ± 0.3	1.5 ± 0.2	0.31 ± 0.03
438	0.098 ± 0.030	3.3 ± 0.3	1.4 ± 0.2	0.25 ± 0.03

Table 4. Cross sections ${}_{20}\sigma_{02}$, ${}_{20}\sigma_{03}$, ${}_{20}\sigma_{04}$ for two-electron capture by He^{2+} ions in collisions with Mg.

Energy (keV amu^{-1})	${}_{20}\sigma_{02}$ (10^{-17} cm^2)	${}_{20}\sigma_{03}$ (10^{-17} cm^2)	${}_{20}\sigma_{04}$ (10^{-17} cm^2)
42.5	2.34 ± 0.19	2.47 ± 0.16	0.17 ± 0.02
47.5	1.37 ± 0.11	1.96 ± 0.12	0.18 ± 0.03
52.5	1.02 ± 0.07	1.84 ± 0.11	0.26 ± 0.03
60.0	0.65 ± 0.05	1.54 ± 0.10	0.24 ± 0.03
70.0	0.45 ± 0.02	1.37 ± 0.08	0.24 ± 0.03
82.5	0.31 ± 0.03	1.24 ± 0.08	0.28 ± 0.04
92.5	0.28 ± 0.03	1.21 ± 0.07	0.34 ± 0.05
108	0.15 ± 0.02	1.12 ± 0.07	0.40 ± 0.05
125	0.12 ± 0.01	1.04 ± 0.06	0.35 ± 0.04
143	0.085 ± 0.011	1.01 ± 0.09	0.34 ± 0.03
163	0.055 ± 0.008	0.82 ± 0.07	0.31 ± 0.04
188	—	0.61 ± 0.05	0.20 ± 0.02
218	—	0.47 ± 0.04	0.18 ± 0.02
250	—	0.32 ± 0.03	0.122 ± 0.014
288	—	0.23 ± 0.03	0.083 ± 0.009
330	—	0.13 ± 0.02	0.053 ± 0.006
380	—	0.068 ± 0.008	0.028 ± 0.003
438	—	0.039 ± 0.005	0.014 ± 0.002

for both one-electron and two-electron capture by He^{2+} obtained from the sums of our measured individual cross sections. These may be compared with the total cross sections measured previously using the oven target approach.

In the case of σ_{10}, the results of DuBois and Toburen (1985), Morgan and Eriksen

Table 5. Cross sections ${}_{20}\sigma_{21}$ and ${}_{20}\sigma_{22}$ for single and double ionization of Mg atoms by He^{2+} impact.

Energy (keV amu^{-1})	${}_{20}\sigma_{21}$ (10^{-15} cm^2)	${}_{20}\sigma_{22}$ (10^{-16} cm^2)
42.5	3.58 ± 0.25	—
47.5	3.38 ± 0.22	—
52.5	3.35 ± 0.18	—
60.0	2.84 ± 0.12	—
70.0	2.39 ± 0.11	—
82.5	2.33 ± 0.12	—
92.5	2.26 ± 0.09	—
107	2.06 ± 0.10	—
125	1.74 ± 0.07	—
143	1.55 ± 0.07	0.20 ± 0.10
163	1.55 ± 0.09	0.56 ± 0.14
188	1.36 ± 0.08	0.74 ± 0.19
218	1.13 ± 0.04	0.76 ± 0.11
250	0.97 ± 0.03	0.90 ± 0.10
288	0.78 ± 0.04	0.91 ± 0.08
330	0.70 ± 0.03	1.15 ± 0.10
380	0.62 ± 0.03	1.31 ± 0.08
438	0.55 ● 0.03	1.42 ± 0.10
500	0.46 ± 0.02	1.37 ± 0.10

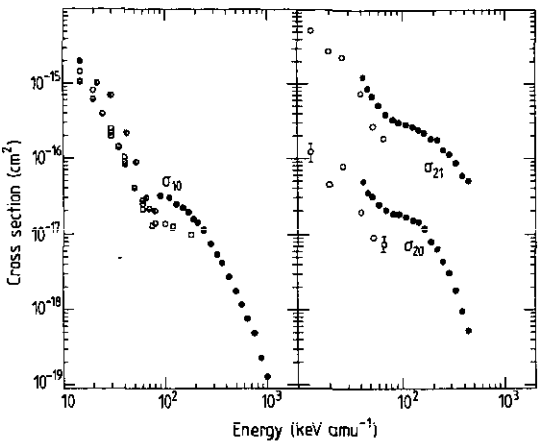

Figure 5. Total cross sections σ_{10} for one electron capture by protons and σ_{21} and σ_{20} for one- and two-electron capture by He^{2+} ions in magnesium. (●), $\sigma_{10} = \Sigma_{10}\sigma_{0n}$, $\sigma_{21} = \Sigma_{20}\sigma_{1n}$ and $\sigma_{20} = \Sigma_{20}\sigma_{0n}$ (present values); ○, σ_{10}, σ_{21}, σ_{20} (DuBois and Toburen 1985); □, σ_{10} (Il'in *et al* 1965); ◐, σ_{10} (Morgan and Eriksen 1979); ⊖, σ_{10} (Berkner *et al* 1969).

(1979), Berkner *et al* (1969) and Il'in *et al* (1965) at energies below 180 keV amu^{-1} exhibit discrepancies and agreement is only within 40%. However, the average value of these previous measurements at our lowest energy of 90 keV amu^{-1} is about a factor of two smaller than our value of σ_{10}. In the same way it can also be seen in figure 5, that values of σ_{21} and σ_{20} for He^{2+} impact measured by DuBois and Toburen (1985) are also about a factor of two smaller than our values in the energy range of overlap.

We believe that the difference between the present total cross sections and those based on the oven target approach reflects at least in part the difficulty in obtaining an accurate determination of effective target thickness. Vapour pressures are strongly dependent on temperature and small errors in temperature determination together with uncertainties in the vapour pressure tables can result in large errors in effective target thickness. Berkner *et al* (1969) have drawn attention to substantial discrepancies of about 40% in published tabulations of vapour pressures for magnesium and, in using the values due to Hultgren *et al* (1963 and additional published data by these authors cited by Berkner *et al* (1969)) (see also Hultgren *et al* (1973)); an uncertainty of 20% was assumed.

As noted earlier, our calibration procedure avoids any reliance on precise temperature measurements and vapour pressure tables. Our measurements were normalized by reference to the values of cross sections for single ionization of Mg by electron impact obtained by Freund *et al* (1990) using a fast crossed beam technique. The fast Mg atom beam flux in these measurements was determined by means of pyroelectric detector, the calibration of which could be checked using known ion beam intensities and by reference to well established electron impact ionization cross sections for both Ar and Kr.

Apart from the differences in magnitude between the present and previously measured total cross sections σ_{10}, the energy dependence of our values can be seen to be consistent with the 'bulge' in the cross section curves apparent in the results of both Il'in *et al* (1965) and DuBois and Toburen (1985) above 80 keV amu^{-1}. The cross section curves for σ_{21} and σ_{20} also exhibit a 'bulge' at high energies.

In figure 6 our cross sections σ_{10} for one-electron capture by protons are shown together with the measured individual contributions ${}_{10}\sigma_{01}$, ${}_{10}\sigma_{02}$ and ${}_{10}\sigma_{03}$. The dominant contribution to σ_{10} can be seen to be provided by the transfer ionization cross section ${}_{10}\sigma_{02}$ corresponding to one-electron capture simultaneous with double ionization. The simple charge transfer cross section ${}_{10}\sigma_{01}$ which has previously been assumed to provide the main contribution to σ_{10} can be seen to be relatively small in the present energy range. The ratio ${}_{10}\sigma_{01}/\sigma_{10}$ varies from 0.24 at 90 keV amu^{-1} to 0.03 at 500 keV amu^{-1}. It is also interesting to note that the transfer ionization cross section ${}_{10}\sigma_{03}$ corresponding to one-electron capture simultaneous with triple ionization exceeds ${}_{10}\sigma_{01}$ at energies above 150 keV amu^{-1}.

In figure 6 we also include cross sections for one-electron capture calculated by Mapleton and Grossbard (1969) using the modified approximate classical theory of Thomas (1927) as previously used by Bates and Mapleton (1967). The total cross sections calculated include captures from all but the 1s subshell into all classically bound states of H while the Mg^+ product ion is assumed to be formed in the ground state. The calculated values therefore do not take full account of all the collision channels. The calculated values can be seen to exceed our measured values of ${}_{10}\sigma_{01}$ but, not surprisingly, fall considerably below our values of σ_{10}. The calculated contributions from the separate 3s, 2p and 2s subshells are also included in figure 6. These indicate that the high energy 'bulge' in the cross section curve for σ_{10}, arises as a result of captures from the 2p and 2s subshells becoming dominant. It is also evident from the energy dependence that such captures involve the transfer ionization processes ${}_{10}\sigma_{02}$ and ${}_{10}\sigma_{03}$ rather more than the simple charge transfer process ${}_{10}\sigma_{01}$.

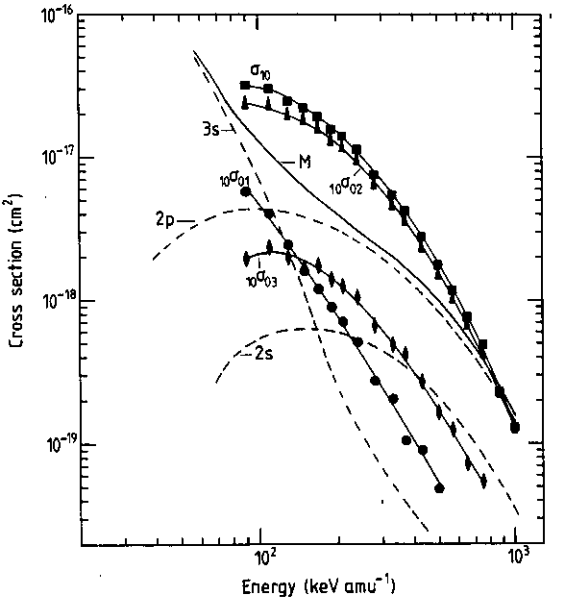

Figure 6. Present cross sections for one-electron capture by H^+ in collisions with Mg compared with theoretical estimates. Lines through the experimental points are simply to guide the eye. ●, ▲, ◆, ${}_{10}\sigma_{01}$, ${}_{10}\sigma_{02}$ and ${}_{10}\sigma_{03}$; ■, $\sigma_{10} = \Sigma\, {}_{10}\sigma_{0n}$; curve *M*, classical total cross sections for one-electron capture calculated by Mapleton and Grossbard (1969) with separate cross sections for one-electron capture from 3s, 2p and 2s subshells of Mg shown as dashed curves.

3.2. Cross sections for electron capture and transfer ionization by H^+ and He^{2+} ions

Our measured individual cross sections for all the processes involving one-electron capture by protons and both one- and two-electron capture by He^{2+} ions are shown in figure 7 together with the low energy results obtained by DuBois (1986). In most cases our cross sections can be seen to be considerably larger than corresponding values due to DuBois (1986) in the energy range of overlap. These discrepancies cannot be explained simply in terms of the different normalization procedures already noted since the two sets of cross sections do not all exhibit the same energy dependence. For proton impact, both sets of data for the dominant ${}_{10}\sigma_{02}$ channel confirm the high energy 'bulge' in the cross section. Both sets of data also show that ${}_{10}\sigma_{01}$ decreases rapidly with increasing energy. However the definite high energy peak in our ${}_{10}\sigma_{03}$ curve is not seen in the results of DuBois (1986).

Individual cross sections for one-electron capture by He^{2+} ions can be seen to be at least a factor of two larger than corresponding values of DuBois (1986). The energy dependence of our high energy values which provide the substantial 'bulge' in σ_{21} (figure 5) seem likely (as in the case of H^+ impact) to reflect substantial contributions from inner shell electron capture. The results in figure 7 show that while the simple charge transfer cross section ${}_{20}\sigma_{11}$ begins to exceed the transfer ionization cross section ${}_{20}\sigma_{12}$ at energies below 47 keV amu^{-1}, it is the transfer ionization cross section ${}_{20}\sigma_{12}$ that provides the dominant contribution to σ_{21} at higher energies. Indeed ${}_{20}\sigma_{11}$ decreases very rapidly with increasing energy and is exceeded by the transfer ionization cross sections ${}_{20}\sigma_{13}$ and ${}_{20}\sigma_{14}$ at energies above 70 and 135 keV amu^{-1} respectively.

In the case of two-electron capture by He^{2+} ions, while the energy dependence of

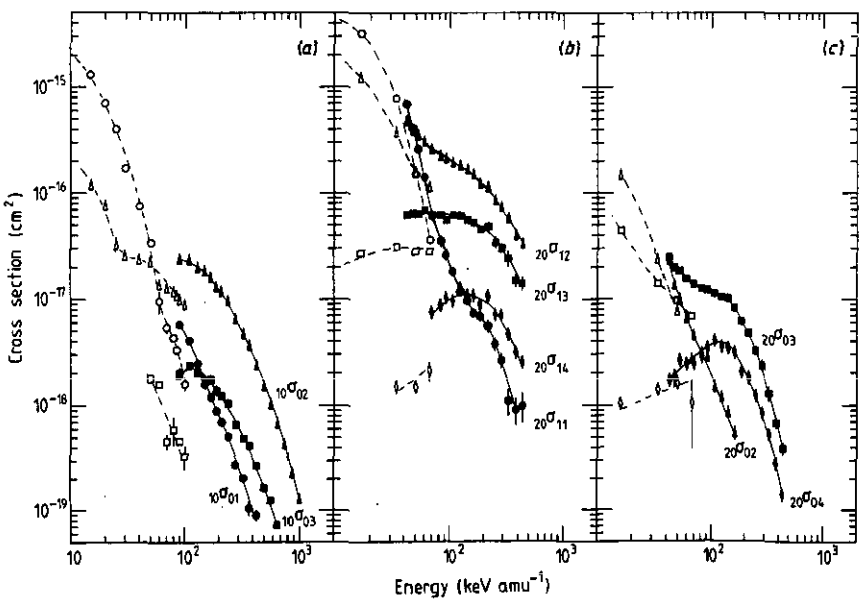

Figure 7. Individual cross sections involving (*a*) one-electron capture by protons, (*b*) one-electron capture by He^{2+} and (*c*) two-electron capture by He^{2+} ions in collisions with Mg atoms. Lines through the experimental points are simply to guide the eye. Full symbols, present values for processes indicated; open symbols, corresponding values due to DuBois (1986).

the curves for ${}_{20}\sigma_{03}$ and ${}_{20}\sigma_{02}$ (figure 7) are similar, the high-energy trend of the results of DuBois (1986) for ${}_{20}\sigma_{04}$ is not confirmed by our values. The high energy 'bulge' in σ_{20} (figure 5) is due mainly to contributions from ${}_{20}\sigma_{03}$ and to a smaller extent ${}_{20}\sigma_{04}$. Our results also show that while the simple two-electron charge transfer cross section ${}_{20}\sigma_{02}$ *becomes equal to the transfer ionization cross section* ${}_{20}\sigma_{03}$ *at our lowest energy* of 43 keV amu^{-1}, at higher energies ${}_{20}\sigma_{03}$ provides the dominant contribution to σ_{20}. Indeed ${}_{20}\sigma_{02}$ is decreasing rapidly with increasing energy and is even exceeded by the transfer ionization cross section ${}_{20}\sigma_{04}$ at energies above about 80 keV amu^{-1}.

3.3. Cross sections for pure ionization by H^+ and He^{2+} impact

In figure 8 cross sections for pure single and double ionization by both H^+ and He^{2+} impact are shown. Low energy cross energy sections for single ionization have been measured by DuBois (1986) with a claimed accuracy of ±50% are included for comparison. His values of ${}_{10}\sigma_{11}$ can be seen to exhibit considerable scatter but are in rough accord with the present values. Values of ${}_{20}\sigma_{21}$ due to DuBois (1986) are only about 0.6 times our values in the energy range of overlap.

The pure single ionization cross sections ${}_{10}\sigma_{11}$ and ${}_{20}\sigma_{21}$, which provide the main contribution to Mg^+ production, are very large and increase with decreasing energy down to our low energy limits. The pure double ionization cross sections ${}_{10}\sigma_{12}$ and ${}_{20}\sigma_{20}$ only exceed the corresponding transfer ionization cross sections (figure 7) ${}_{10}\sigma_{02}$ and ${}_{20}\sigma_{12}$ at high impact energies. As noted earlier, Mg^{3+} and Mg^{4+} production through pure ionization is insignificant compared with transfer ionization in the present energy range.

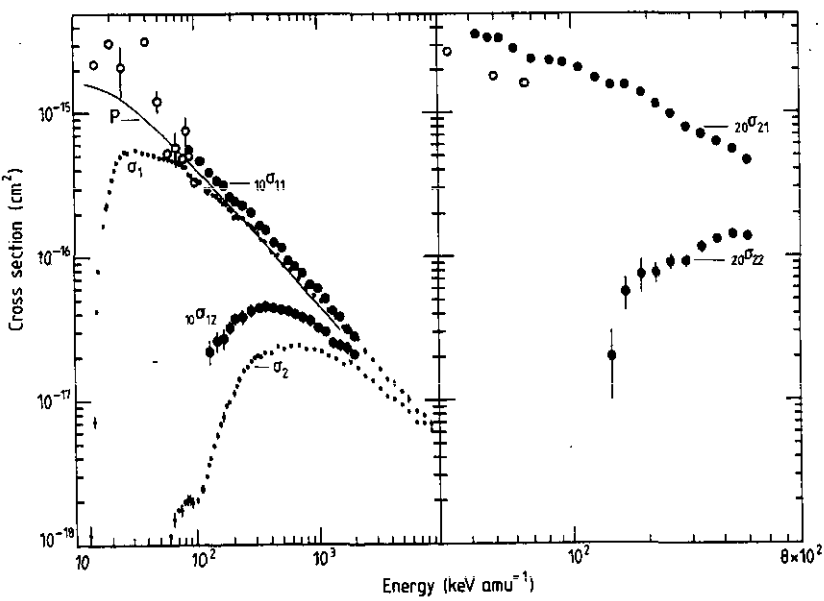

Figure 8. Cross sections for single and double ionization ofmagnesium. ●, ${}_{10}\sigma_{11}$ and ${}_{10}\sigma_{12}$ for H^+ impact and ${}_{20}\sigma_{21}$ and ${}_{20}\sigma_{22}$ for He^{2+} impact (present results); ○, ${}_{10}\sigma_{11}$ and ${}_{20}\sigma_{21}$ for H^+ and He^{2+} impact (DuBois 1986); σ_1, σ_2, cross sections for single and double ionization by electrons: (McCallion *et al* 1992); curve *P*, cross sections for removal of electrons from 3s+2p subshells calculated by Peach (1970).

For H^+ impact, our cross sections may also be compared with our recently measured cross sections σ_1 and σ_2 for single and double ionization by equivelocity electrons (McCallion *et al* 1992). As expected, cross sections ${}_{10}\sigma_{11}$ can be seen to become equal to σ_1 at our high velocity limit of 2 MeV amu^{-1}. The low energy structure in σ_2 is believed to be (cf Peach 1970) due to an Auger transition following removal of a 2p electron and this process results in comparatively large values of σ_2 which approach σ_1 at high velocities. For ion impact such a well defined structure is not expected or observed in ${}_{10}\sigma_{12}$ within the present more limited velocity range. It can be seen that values of ${}_{10}\sigma_{12}$ are approaching ${}_{10}\sigma_{11}$ more quickly at high velocities than the corresponding cross sections for electron impact. Peach (1970) has used the Born approximation to calculate proton impact cross sections for the removal of the outer 3s electron together with a 2p inner shell electron. These (3s+2p) electron removal cross sections (figure 8) can be seen to be about 0.87 times our values of ${}_{10}\sigma_{11}$ with the same energy dependence down to our lowest energy of 90 keV amu^{-1}.

Cross sections ${}_{20}\sigma_{21}$ and ${}_{20}\sigma_{22}$ for He^{2+} impact (figure 8) can be seen to be larger than corresponding values for proton impact. Cross sections ${}_{20}\sigma_{22}$ appear to be attaining a peak value at about 450 keV amu^{-1} where corresponding cross sections ${}_{10}\sigma_{12}$ for proton impact also maximize. In figure 9 we illustrate that our measured cross sections ${}_{20}\sigma_{21}$ for single ionization by He^{2+} impact are well described by Z^2 times (where the atomic number $Z=2$) the corresponding proton impact cross sections at our highest velocities in accordance with simple Born approximation predictions. However, rather surprisingly Z^2 scaling also appears to be satisfactory at the lowest velocities we consider.

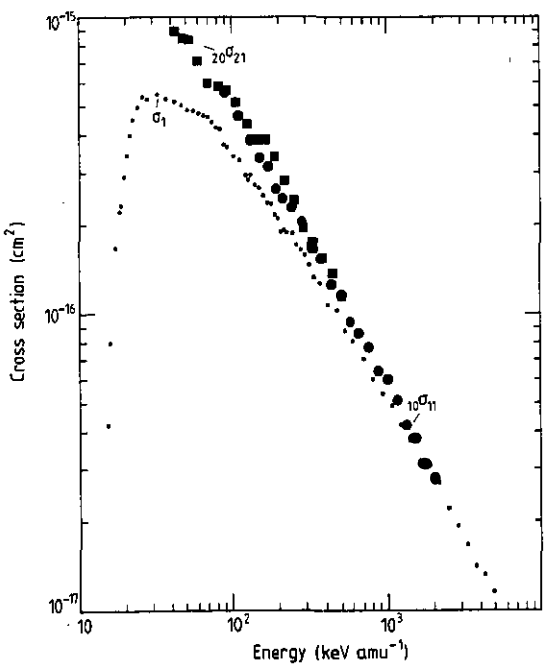

Figure 9. Energy dependence of single ionization cross section ratio σ/Z^2. ■, ${}_{20}\sigma_{21}$ for He^{2+} impact; ●, ${}_{10}\sigma_{11}$ for H^+ impact; σ_1, electron impact.

4. Conclusions

Ion–ion and electron–ion coincidence counting techniques have been used to determine individual cross sections for the main processes which involve both ionization and one-electron capture in collisions of H^+ with Mg, and both ionization, one and two-electron capture in collisions of He^{2+} with Mg at energies within the respective ranges 90–2000 and 43–500 keV amu^{-1}. Processes leading to Mg^{n+} ions for n up to 4 have been considered. At these high energies there is evidence that, in addition to the outer 3s electron, inner shell 2s and 2p electrons are important. Some substantial differences between our results and some previous lower energy data based on the use of ion–ion coincidence counting by DuBois (1986) are believed to reflect, at least in part, the use of different normalization procedures. The present measurements have been normalized to known cross sections for single ionization of Mg by electron impact rather than to total electron capture cross sections based on the oven target method where accurate target thickness determination is difficult.

Cross sections for pure single ionization by both H^+ and He^{2+} impact provide the main contribution to Mg^+ production in the present energy range. Mg^{2+} is formed mainly by pure ionization at high impact energies and by transfer ionization at the lower energies. Mg^{3+} and Mg^{4+} ions are formed by transfer ionization processes. The main contributions to both one- and two-electron capture are also found to be provided by transfer ionization processes.

Acknowledgments

This work is part of a programme supported by a Rolling Grant from the Science and Engineering Research Council. One of us (YI) was able to take part in these measurements as a result of support from the Japanese Ministry of Education.

References

Bates D R and Mapleton R A 1967 *Proc. Phys. Soc.* **90** 909
Berkner K H, Pyle R V and Stearns J W 1969 *Phys. Rev.* **178** 248
DuBois R D 1986 *Phys. Rev.* A **34** 2738
DuBois R D and Toburen L H 1985 *Phys. Rev.* A **31** 3603
Freund R S, Wetzel R C, Shul R J and Hayes T R 1990 *Phys. Rev.* A **41** 3575
Hultgren R R, Orr R L, Anderson P D and Kelly K K 1963 *Selected Values of Thermodynamic Properties of Metals and Alloys* (New York: Wiley)
Hultgren R R, Dlsai P D, Hawkins D T, Gleiser M, Kelly K K and Wagman D D 1973 *Selected Values of Thermodynamic Properties of The Elements* (Cleveland, OH: American Society for Metals)
Il'in R N, Oparin V A, Solov'ev E S and Fedorenko N V 1965 *JETP Lett* **2** 197
Mapleton R A and Grossbard N 1969 *Phys. Rev.* A **188** 228
McCallion P, Shah M B and Gilbody H B 1992 *J. Phys. B: At. Mol. Opt. Phys.* **25** 1051
Morgan T J and Eriksen F J 1979 *Phys. Rev.* A **19** 1448
Peach G 1970 *J. Phys. B: At. Mol. Phys.* **3** 328
Shah M B, Elliott D S and Gilbody H B 1987 *J. Phys. B: At. Mol. Phys.* **20** 3501
Shah M B and Gilbody H B 1981 *J. Phys. B: At. Mol. Phys.* **14** 2361
—— 1982 *J. Phys. B: At. Mol. Phys.* **15** 3441
—— 1983 *J. Phys. B: At. Mol. Phys.* **16** 4395
Thomas L H 1927 *Proc. R. Soc.* A **114** 561